Cardiovasc Toxicol (2010) 10:51–65
DOI 10.1007/s12012-010-9062-2

Nitrogen Compounds Prevent H9c2 Myoblast Oxidative Stress-Induced Mitochondrial Dysfunction and Cell Death

João P. Silva · Vilma A. Sardão · Olga P. Coutinho · Paulo J. Olveira

Published online: 30 January 2010

Abstract Oxidative stress has been connected to various forms of cardiovascular diseases. Previously, we have been investigating the potential of new nitrogen-containing synthetic compounds using a neuronal cell model and different oxidative stress conditions in order to elucidate their potential to ameliorate neurodegenerative diseases. Here, we intended to extend these initial studies and investigate the protective role of four of those new synthetic compounds (FMA4, FMA7, FMA762 and FMA796) against oxidative damage induced to H9c2 cardiomyoblasts by *tert*-butylhydroperoxide (*t*-BHP). The data indicates that FMA762 and FMA796 decrease *t*-BHP-induced cell death, as measured by both sulforhodamine B assay and nuclear chromatin condensation evaluation, at non-toxic concentrations. In addition, the two mentioned compounds inhibit intracellular signalling mechanisms leading to apoptotic cell death, namely those mediated by mitochondria, which was confirmed by their ability to overcome *t*-BHP-induced morphological changes in the mitochondrial network, loss of mitochondrial membrane potential, increased expression of the pro-apoptotic proteins p53, Bax and AIF and activation of caspases-3 and -9. Importantly, our results indicate that the compounds' ROS scavenging ability plays a crucial role in the protection profile, as a significant decrease in *t*-BHP-induced oxidative stress occurred in their presence. Data obtained indicates that some of the test compounds may clearly prove valuable in a clinical context by diminishing cardiac injury associated to oxidative stress without any toxicity.

Keywords Nitrogen compounds · Cardiac oxidative stress · H9c2 myoblasts · Mitochondria · Apoptosis

Abbreviations

ROS	Reactive oxygen species
t-BHP	*tert*-butyl hydroperoxide
SRB	Sulforhodamine B
TMRM	Tetramethyl rhodamine methyl ester
$\Delta\psi$	Membrane potential
CCCP	Carbonyl cyanide *m*-chloro phenyl hydrazone
AIF	Apoptosis-inducing factor
CM-H_2DCFDA	5-(and-6)-chloromethyl-2′,7′-dichlorodihydrofluorescein diacetate
NBT	NitroBlue Tetrazolium
fSD	Intracellular fluorescence standard deviation

J. P. Silva (✉) · O. P. Coutinho
CBMA—Molecular and Environmental Biology Centre, Department of Biology, University of Minho, Campus de Gualtar, 4710-057 Braga, Portugal
e-mail: jpsilva@bio.uminho.pt

V. A. Sardão · P. J. Olveira
Center for Neurosciences and Cellular Biology, University of Coimbra, Coimbra, Portugal

Introduction

Cardiovascular diseases have been established as one of the leading causes of death worldwide [1]. By its turn, oxidative stress has been associated to various forms of cardiovascular diseases, including atherosclerosis, ischaemia–reperfusion injury and other cardiomyopathies [2, 3].

Supporting the connection between oxidative stress and cardiac pathologies, it has been demonstrated that the administration of exogenous antioxidants results in the protection against oxidative myocardial injury [4, 5].

Mitochondria are recognized as the major sites of ROS production in the cell, since about 2% of total oxygen escapes the electron transport chain, leading to the formation of superoxide radicals and subsequently other reactive species, such as hydrogen peroxide and hydroxyl radicals [6]. Since cardiac tissue is very abundant in mitochondria (up to 35% of the cell volume) and the cardiac muscle is dependent on a continuous supply of oxidative phosphorylation-derived ATP [7], cardiac cells are at a high risk of suffering oxidative damage.

The production of ROS by mitochondria seems to be also involved in the initiation and execution of apoptotic cell death [1] and apoptosis has been associated with human cardiovascular system impairment [8]. ROS can promote cytochrome c release from mitochondria to the cytosol, probably by a mechanism involving the mitochondrial permeability transition (MPT) pore, which involves swelling of the mitochondrial matrix and rupture of the outer membrane [9]. Alternatively, cytochrome c may also be released in a MPT-independent way, regulated by some members of the Bcl-2 proteins' family, with consequent downstream activation of caspases, thus playing an important role in the overall regulation of cardiomyocyte apoptosis [10]. Therefore, pharmacological agents that would be able to effectively suppress ROS formation and modulate mitochondrial function, with minimal intrinsic toxicity, should deserve a more intense investigation [1, 4].

We have previously described the potential of new nitrogen compounds from organic synthesis, against different conditions in which oxidative stress is involved [11, 12]. Four of them (named FMA4, FMA7, FMA762 and FMA796) showed an elevated ROS scavenging activity in a neuronal cell model, which resulted in lipid peroxidation and oxidative DNA damage protection.

In the present study, the hypothesis was to extend the benefit of these new compounds to cardiac cells, which differ from other cell types by their antioxidant networks [13] and their limitation in accumulating antioxidants [14]. If protection is obtained with the test compounds, new perspectives could be open for their clinical use. Of particular interest was the assessment of their potential activity at the mitochondrial level.

A clonal myogenic cell line derived from embryonic rat ventricle (H9c2 cells) was used as biological model, and the pro-oxidant *tert*-butylhydroperoxide (*t*-BHP) was chosen as the oxidative stress inducer. The system has been extensively used in the literature to study molecular responses of cardiomyocytes to oxidative damage.

Materials and Methods

Chemicals

The test compounds used in this study (Fig. 1) were prepared in the group of Organic Synthesis, Chemistry Department, University of Minho, from the reaction of an appropriate phenolic aldehyde with a substituted amine, following an experimental procedure adapted from previous work [15]. The compounds were provided as a yellowish powder, which was reconstituted in DMSO, aliquoted and maintained frozen at −80°C until use. Each aliquot was thawed only once. The new molecules have a phenol ring with hydroxyl groups (Fig. 1) that are usually responsible for the antioxidant properties of a compound. On the other hand, it is also known that compounds with nitrogen groups can easily interact with active centres responsible for different functions in living organisms. Therefore, the association of these two moieties in the same molecule was expected to result in new structures with increased antioxidant potential and greater ability to stabilize free radicals, in comparison with the molecules traditionally used [15].

Foetal bovine serum (FBS) was obtained from Bio-Chrom KG (Berlin, Germany); Dulbecco's Modified Eagle's Medium (DMEM) cell culture medium, dimethyl sulfoxide (DMSO), EDTA, trypsin, *tert*-butyl hydroperoxide, sulforhodamine, phenazine methosulphate (PMS), reduced nicotinamide adenine dinucleotide (NADH), NitroBlue Tetrazolium (NBT) and Hoechst 33342 were purchased from Sigma–Aldrich (St. Louis, MO, USA). Tetramethyl rhodamine methyl ester (TMRM), Calcein-AM and 5-(and-6)-chloromethyl-2′,7′-dichlorodihydrofluorescein diacetate (CM-H_2DCFDA) were obtained from Invitrogen (Eugene, OR, USA).

H9c2 Cell Culture

H9c2 cell line was originally derived from embryonic rat heart tissue using selective serial passages [16] and was purchased from America Tissue Type Collection (Manassas, VA, USA). This cell line has shown electrophysiological and biochemical properties of both skeletal and cardiac tissues, including depolarization in response to acetylcholine and rapid activation of calcium currents through L-type channels. They have been used extensively in the literature as models for cardiomyoblasts and have been considered as a proper model to study molecular responses of the cardiomyocyte to oxidative damage [17, 18]. Cells were grown in DMEM supplemented with 1.5 g l^{-1} sodium bicarbonate, 10% FBS, 100 U ml^{-1} of penicillin and 100 μg ml^{-1} of streptomycin in 75-cm^2 tissue culture flasks, and maintained at 37°C, in a humidified incubator containing 5% CO_2.

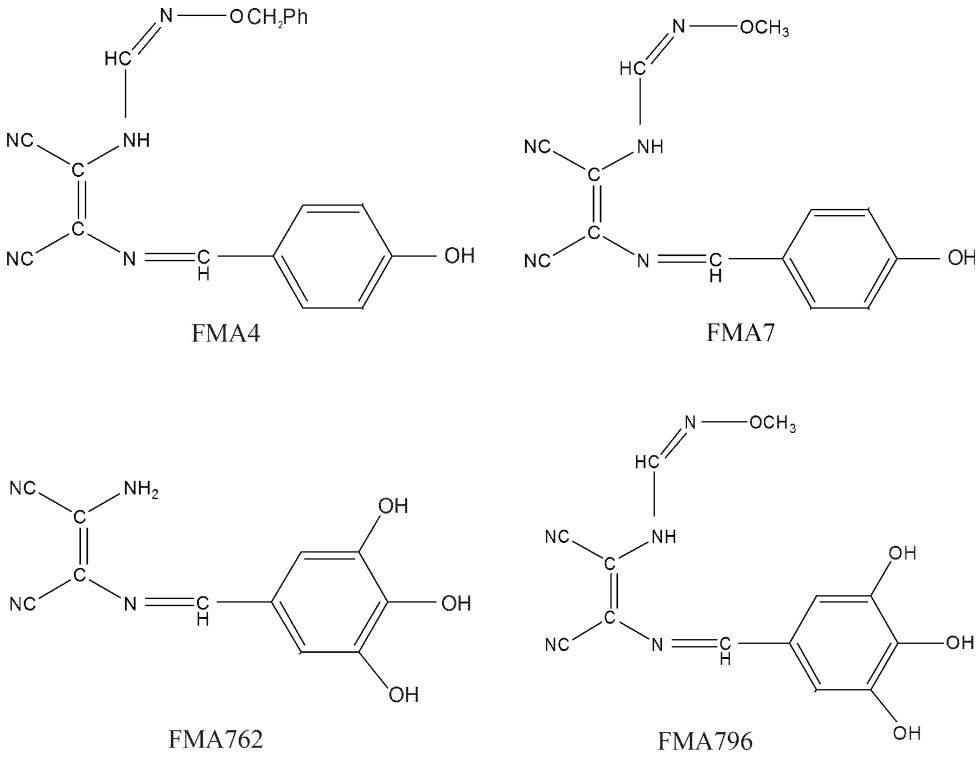

Fig. 1 Schematic structure of the newly synthesized nitrogen compounds. A phenolic unit is linked to an amine function through a linear chain containing a nitrogen atom in three carbon atoms. FMA762 and FMA796 differ mainly from FMA4 and FMA7 by the presence of three hydroxyl groups within the phenol ring, instead of one. The compounds were prepared by F. M. Areias, Group of Organic Chemistry, University of Minho

To prevent loss of differentiation potential, cells were not allowed to become confluent. So, they were fed every 2–3 days, and sub-cultured once they reached 70–80% confluence, by treatment with a 0.05% trypsin/EDTA solution. Cells were seeded at a density of 35000 cells per ml, either in 24-well plates (final volume of 1 ml well^{-1}) for sulforhodamine B assays, or in 100 mm diameter tissue culture dishes for Western blots. For experiments using fluorescence microscopy, cells were seeded as described previously, but in 6-well plates containing glass coverslips (final volume of 2 ml medium well^{-1}). Treatment with both compounds in study and *t*-BHP was done for either 3 or 6 h, as mentioned in the captions of figures.

Sulforhodamine B (SRB) Assay

The effects of the nitrogen compounds on cell proliferation per se and on the protection against *t*-BHP-induced cell death was evaluated by the sulforhodamine B assay, according to Papazisis et al. [19], with slight modifications [20]. H9c2 cells were seeded in 24-well plates and treated with the nitrogen compounds in different time points, in the presence or absence of *t*-BHP. Following this treatment, the incubation medium was removed and cells were washed with PBS and fixed in ice cold methanol, containing 1% acetic acid, for at least 1 h. Cells were then incubated with 0.5% (w v^{-1}) sulforhodamine B dissolved in 1% acetic acid for 1 h at 37°C. Unbound dye was removed by washing several times with 1% acetic acid. Bound SRB was then solubilized with 10 mM Tris base solution, pH 10. After shaking the plates to dissolve the SRB, 200 µl from each well was transferred to 96-well plates and the absorbance read at 540 nm, against a blank containing 10 mM Tris alone. Results were expressed relatively to $t = 0$ h, in the presence of the vehicle alone (DMSO), which was considered as 100% of cell proliferation/cell viability.

Chromatin Condensation Detection

The morphology of cells nuclei was observed by using the cell-permeable DNA dye Hoechst 33342. Cells presenting nuclei homogeneously stained with the dye were considered to be normal, whereas the ones presenting chromatin condensation were considered as apoptotic.

In brief, after being treated with the compounds in the presence of *t*-BHP, cells were carefully washed with PBS, fixed with 2 ml of ice-cold absolute methanol and stained with 1 µg ml^{-1} of Hoechst 33342 for 30 min, at 37°C, in the dark. Nuclear morphological changes were detected in a fluorescence microscope (Zeiss Axioskop 2 plus) with an UV filter. Two hundred cells from several randomly chosen fields were counted and the number of apoptotic cells expressed as a percentage of the total number of cells.

Triple Labelling of H9c2 Cells with TMRM, Hoechst 33342 and Calcein-AM

H9c2 cellular and mitochondrial morphological changes were analysed by fluorescence microscopy, according to Sardão et al. [20], with slight modifications. Briefly, cells adhered to coverslips placed in the bottom of 6-well plates and treated with the compounds in the presence of *t*-BHP, were incubated with 100 nM tetramethyl rhodamine methyl ester (TMRM), 1 μg ml^{-1} Hoechst 33342 and 300 nM Calcein-AM for 30 min, at 37°C, in the dark. Coverslips were then carefully removed and cells observed under a fluorescence microscope.

Measurement of Mitochondrial Membrane Potential ($\Delta\psi$)

Monitorization of the mitochondrial $\Delta\psi$ was performed by loading cells with TMRM, a membrane-permeable cationic fluorophore that accumulates electrophoretically inside mitochondria, proportionally to their $\Delta\psi$ [21]. Thirty minutes before the end of the 3-h incubation period with 50 μM *t*-BHP and the nitrogen compounds, TMRM was added to the cell culture medium, to a final concentration of 100 nM. Cells were then visualized under a fluorescence microscope, using the adequate filter setting. As described elsewhere, mitochondrial TMRM labelling results into large fluorescence standard deviation (fSD) values between the mitochondrial bodies (high fluorescence) and cytosol (dark background). An initial slight mitochondrial depolarization causes the redistribution of TMRM from mitochondria into the cytosol, resulting in practically no alterations in the mean cell fluorescence value, although the fSD is altered. A large-scale depolarization causes a dramatic decrease in the fSD as the dye is evenly distributed throughout the cell [22]. So, in addition to cell mean fluorescence, we have also quantified fSD for each treatment, which is recognized to be a more sensitive parameter of quantification. Both cell mean fluorescence intensity and the fSD were quantified using ImageJ 1.40 g software (National Institutes of Health, USA). As a test control, cells were subjected to complete mitochondrial depolarization by treatment with 50 μM carbonyl cyanide *m*-chloro phenyl hydrazone (CCCP).

Preparation of Total Protein Extracts and Nuclear Fractionation

To obtain total protein extracts, after treatment with the compounds in the presence of *t*-BHP, H9c2 cells were harvested by trypsinization and centrifuged twice at $1000\times g$, for 5 min. Floating cells were also collected and combined with the adhered ones. Cellular pellets were then resuspended in 50 μl of lysis buffer (20 mM HEPES/NaOH, pH 7.5, 250 mM Sucrose, 10 mM KCl, 2 mM $MgCl_2$, 1 mM EDTA) supplemented with 2 mM dithiothreitol (DTT), 100 μM phenylmethylsulfonyl fluoride (PMSF) and a protease inhibitor cocktail (containing 1 μg ml^{-1} of leupeptin, antipain, chymostatin and pepstatin A). Afterwards, pellets were disrupted with ~30 passages through a 27-gauge needle. The cell suspension was then rapidly frozen/thawed three times in liquid nitrogen and kept at −80°C until use.

For the preparation of nuclear fractions, cells were harvested as described previously and resuspended in homogenization buffer (250 mM sucrose, 20 mM HEPES/KOH, pH 7.5, 10 mM KCl, 1.5 mM $MgCl_2$, 0.1 mM EDTA, 1 mM EGTA) supplemented with 1 mM DTT, 100 μM PMSF and protease inhibitor cocktail (containing 1 μg ml^{-1} of leupeptin, antipain, chymostatin and pepstatin A). Cells were then homogenized in a Potter–Elvehjem homogeniser with a Teflon pestle and the homogenate was centrifuged at $220\times g$, for 5 min, at 4°C. The pellet was resuspended in 50 μl of a 250 mM sucrose/10 mM $MgCl_2$ buffer, and the resulting suspension was carefully poured over 500 μl of another buffer containing 350 mM sucrose/0.5 mM $MgCl_2$, in order to form a gradient. These gradients were then centrifuged at ~$1271\times g$, for 5 min, at 4°C and the pellets resuspended in 50 μl of the 350 mM sucrose/0.5 mM $MgCl_2$ buffer.

The amount of protein in each sample was determined by the Bradford method, using bovine serum albumin (BSA) as standard.

Determination of Caspase-Like Activity

The activities of caspases 3 and 9 were assessed spectrophotometrically by determining the cleavage of the respective colorimetric substrate, as described by Serafim et al. [23]. Briefly, after treating cells with the compounds for 3 h, total protein extracts were obtained according to the procedure described previously, and a sample volume corresponding to 25 and 50 μg of protein for caspase-3 and caspase-9, respectively, was added to the reaction buffer (0.1% CHAPS, 10% Sucrose, 25 mM HEPES, pH 7.5, supplemented with 10 mM DTT). The enzymatic reactions, in a final volume of 200 μl, were initiated by the addition of the colorimetric substrates Ac–DEVD–*p*NA, for caspase-3-like protease activity, and Ac–LEHD–*p*NA, for caspase-9-like protease activity, to a final concentration of 100 μM. After 2 h incubation at 37°C, in the dark, 100 μl from each sample was transferred to a 96-well plate and the reaction product (nM μg^{-1} protein) measured spectrophotometrically at 405 nm. A calibration with known concentrations of *p*-nitroanilide (*p*NA) was done.

Western-Blot Analysis

Protein expression was determined by Western-blot. Equal amounts of protein (50 μg) were denatured in sample loading buffer, separated in 8–15% polyacrylamide gels by sodium dodecyl sulphate–polyacrylamide gel electrophoresis (SDS/PAGE), and transferred to polyvinylidene difluoride (PVDF) membranes (Amersham Biosciences, Buckinghamshire, UK). The membranes were blocked for 2 h, at room temperature, in TPBS (PBS and 0.1% Tween 20, pH 7.4), containing 5% skim milk. Blots were then incubated overnight, at 4°C, with goat anti-p53 (1:200, Santa Cruz Biotechnology, CA, USA), rabbit anti-Bax (1:8000, Cell Signaling Technology, Beverly, MA, USA), rabbit anti-AIF (1:1000, Cell Signaling Technology) or mouse anti-β-actin (1:10000, Sigma–Aldrich, St. Louis, MO, USA). All primary antibodies were diluted in TPBS containing 1% BSA. After three washes, membranes were incubated for 1 h in the presence of the horseradish peroxidase-conjugated anti-goat immunoglobulin (IgG) for p53 (1:5000, DAKO Cytomation, Denmark), anti-mouse immunoglobulin (IgG) for β-actin (1:10000, Amersham) and anti-rabbit immunoglobulin (IgG) for the other proteins (1:10000, Amersham). Immunoreactive bands were then detected using the Immobilon chemiluminescence detection kit (Millipore, Billerica, MA, USA). The bands were visualized by using a molecular imager Chemi-Doc XRS system (Bio-Rad, Hercules, CA, USA), and the images were analysed with the Quantity One software (Bio-Rad). Band intensity for p53, Bax and AIF was normalized against the loading control β-actin.

Detection of Intracellular Reactive Oxygen Species

Intracellular ROS formation was assessed by using the non-fluorescent probe 5-(and-6)-chloromethyl-2′,7′-dichlorodihydrofluorescein diacetate (CM-H_2DCFDA), which permeates cell membrane and becomes oxidized in the presence of ROS, yielding the fluorescent 2,7′-dichlorofluorescein (DCF), by a method previously described [21], slightly modified. Briefly, after a 3-h treatment with *t*-BHP and the nitrogen compounds, cells in coverslips were incubated with 7.5 μM CM-H_2DCFDA for 30 min, at 37°C, in the dark. Cells were then observed by fluorescence microscopy using a fluorescein filter in a Leica DM 4000B microscope. The intracellular mean fluorescence intensity was quantified using the ImageJ 1.40 g software (National Institutes of Health, USA).

Evaluation of Superoxide Radical Scavenging Activity

The superoxide radical scavenging activity of the compounds was determined in a cell-free system, by using both a non-enzymatic and an enzymatic system, as previously described [24], which is based on the reduction, at 560 nm, of Nitroblue Tetrazolium (NBT) to the blue chromogen formazan, by $O_2^{\bullet -}$.

In the non-enzymatic assay, superoxide radicals were generated by the phenazine methosulphate (PMS)/NADH system. Briefly, increasing concentrations of the nitrogen compounds (1–100 μM) were added, in a 96-well plate, to a reaction mixture consisting of 166 μM NADH and 43 μM NBT. Reactions were then initiated by the addition of 2.7 μM PMS, to a final volume of 300 μl, and followed spectrophotometrically for 2 min, at room temperature. All reagents were dissolved in 19 mM phosphate buffer, pH 7.4.

In the enzymatic assay, the system xanthine/xanthine oxidase (X/XO) was used to produce the superoxide anion. Reaction mixtures in the wells consisted of 44 μM xanthine (dissolved first in 1 μM NaOH and then in 50 mM phosphate buffer with 0.1 mM EDTA, pH 7.8), 50 μM NBT (dissolved in 50 mM phosphate buffer with 0.1 mM EDTA, pH 7.8) and the nitrogen compounds, tested at different concentrations (0.25–100 μM). Enzymatic reactions were initiated by the addition of 0.29 U ml^{-1} XO (dissolved in 0.1 mM EDTA), to a final volume of 300 μl, and the reduction of NBT followed spectrophotometrically for 2 min, at room temperature.

IC_{50} values were determined, for each assay, from the dose–response curves obtained for each compound, as the concentrations required inhibiting the reduction of NBT in 50%.

Statistical Analysis

Data is expressed as the mean ± SEM, of the indicated number of experiments. The significance of the differences between the means observed was evaluated using the unpaired two-tailed Student's *t*-test or the one-way ANOVA followed by the Student–Newman–Keuls post hoc test. A difference of $P \leq 0.05$ was considered significant.

Results

Effects of the Compounds on Cell Proliferation

The sulforhodamine B assay was used to assess the effect of the compounds per se on cell proliferation in a time and dose-dependent manner. As it can be observed in Fig. 2, at the concentrations tested, none of the compounds alone seem to affect cellular proliferation, at least up to 96 h in culture. Despite the absence of statistical significance, concentrations higher than 40 μM of FMA762 and

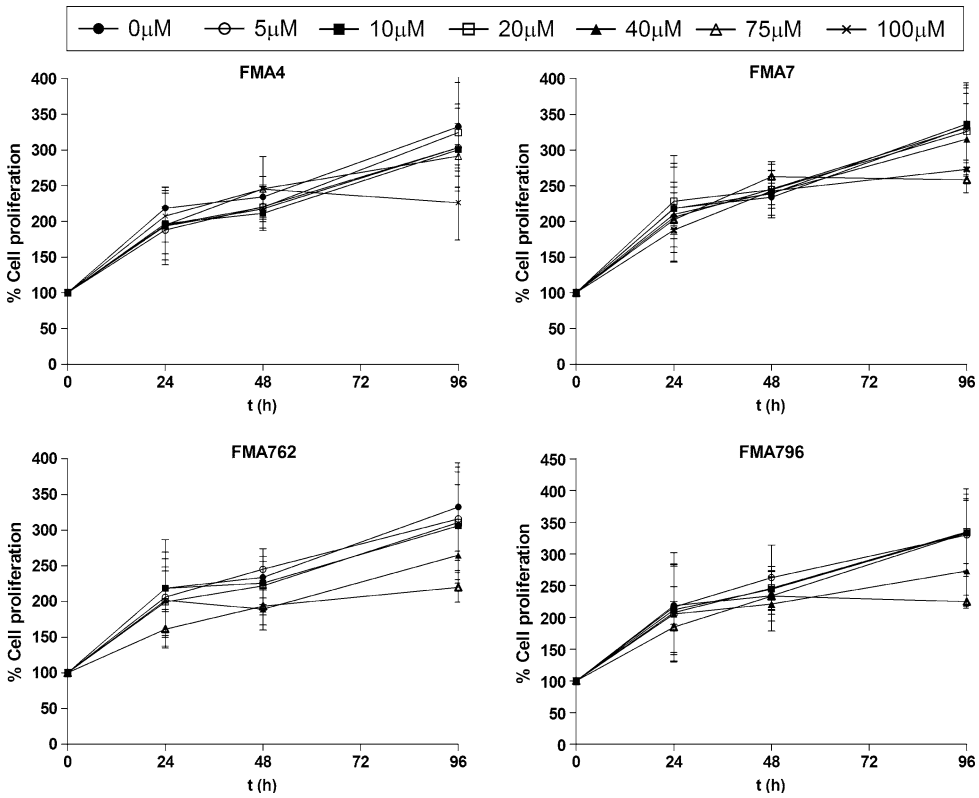

Fig. 2 Cellular proliferation assessed with the sulforhodamine B assay. H9c2 cells proliferation was followed up to 96 h, in the presence of different compounds concentrations, as indicated. The percentage of cellular proliferation was calculated relatively to $t = 0$ h. Proliferation in control cells (no test compounds) was assessed in the presence of 0.1% DMSO. For each concentration, the mean ± S.D. for at least three independent experiments is represented. No statistically significant differences were found between the different concentrations shown and the respective controls for each time point

FMA796 caused a small inhibition of cell growth, hence those concentrations were not used in subsequent assays. For 100 μM, there is some effect for these two compounds in cell proliferation, although toxicity was still not observed (data not shown).

The next step was to verify if any of the test compounds could afford protection against the loss of cells caused by *t*-BHP-induced toxicity on H9c2 cells. The thiol-oxidizing agent *t*-BHP is metabolized intracellularly, generating *tert*-butoxyl radicals, and has been commonly used as an inducer of oxidative stress in several cell models, leading among other effects to a decrease in reduced glutathione [25, 26]. Depending on the cell line used, results obtained have also shown that this deleterious agent may also induce several characteristics of cell apoptosis, namely at mitochondrial level [6]. Based on the proliferation curves obtained, the concentrations of compounds used in the following experiments were chosen, namely 20 and 40 μM for FMA4 and FMA7, and 5 and 20 μM for FMA762 and FMA796. It should be noted that the lower concentrations tested (20 μM for FMA4 and FMA7, and 5 μM for FMA762 and FMA796) correspond to the approximate IC_{50} values previously determined by the DPPH discolouration assay. Moreover, all the concentrations chosen had previously shown high levels of protection against oxidative damage induced to PC12 cells [11, 12].

Data in Fig. 3 indicate that after a 6-h treatment with *t*-BHP, a decrease of about 55% in cell numbers occurs, in comparison with control cells. However, this decrease was prevented, in a statistically significant manner, in the presence of the compounds, except for FMA4. The protection observed with FMA762 and FMA796, besides being more powerful, is also attained for a lower concentration (5 μM). This superior protective effect of FMA762 and FMA796 against *t*-BHP-induced toxicity is in accordance with our previous results, obtained in PC12 cells [12].

Chromatin Condensation

Chromatin condensation is a hallmark of apoptosis. To verify if the protection against the cytotoxicity induced by *t*-BHP involves inhibition of this apoptotic phenomenon, H9c2 cells were stained with the fluorescent probe Hoechst 33342, which binds to DNA, and visualized under an epifluorescence microscope to quantify nuclei with typical apoptotic morphology.

Figure 4 shows that the treatment with *t*-BHP leads to a statistically significant increase in the number of nuclei with condensed chromatin, which occurs in a time-dependent manner. When the nitrogen compounds were co-incubated with *t*-BHP, decreased numbers of apoptotic cells occurred.

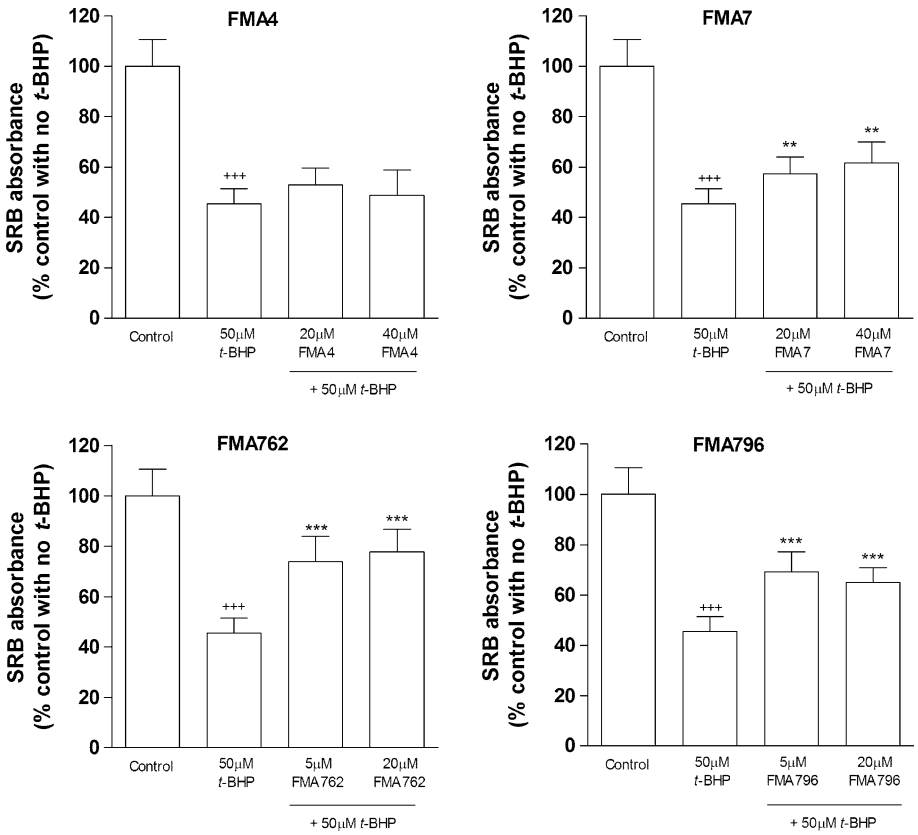

Fig. 3 Effects of the compounds on the reduction in cell viability induced by 50 μM *t*-BHP, evaluated by the sulforhodamine B assay. H9c2 cells were incubated for 6 h in the presence of the nitrogen compounds and *t*-BHP. Results are presented in terms of percentage of cell viability, determined relatively to the control containing only 0.1% DMSO, which was considered as representing 100% of viability. For each bar, the mean ± SEM for at least three independent experiments is represented. $^{+++}$ $P \leq 0.001$, compared to control cells (DMSO); ** $P \leq 0.01$, *** $P \leq 0.001$, when compared to 50 μM *t*-BHP

Co-incubation with FMA762 and FMA796 resulted in almost a complete inhibition in the formation of apoptotic nuclei (Fig. 4). The data suggests that the protection afforded by the test compounds against loss of cells (Fig. 3) also results from inhibition of apoptosis.

Vital Imaging of H9c2 Cells Labelled with TMRM, Hoechst 33342 and Calcein-AM

In order to identify possible morphological alterations induced by *t*-BHP, a triple labelling with TMRM, Calcein-AM and Hoechst 33342 was used. TMRM is a cationic, mitochondrial selective probe that is accumulated by that organelle in a membrane potential ($\Delta\psi$)-dependent manner. Calcein-AM readily passes through the cell membrane of viable cells because of its high hydrophobicity. After it permeates into the cytoplasm, calcein-AM is hydrolyzed by esterases to calcein, which remains inside the cells and emits green fluorescence. Thus, the accumulation of this probe inside the cells is indicative of membrane integrity, since damaged cell membrane in necrotic cells prevents calcein from accumulating intracellularly. Hoechst, as mentioned previously, binds to DNA and is commonly used to visualize nuclei, allowing the observation of chromatin condensation or other nuclear alterations, in apoptotic cells.

After the data pictured in Fig. 3, 3 h of incubation with *t*-BHP was chosen in order to detect alterations that may precede widespread cell death. Representative images in Fig. 5 show that control (untreated cells) exhibit polarized mitochondria distributed throughout the cytoplasm (A and B), are strongly labelled by calcein (C) and show well-defined nuclei, with normal chromatin distribution (D). On the other hand, cells treated with *t*-BHP displayed several morphological changes, which include a much smaller size, resulting from rounding up (A) and loss of the mitochondrial polarization (B). Some cells presented other features, such as a weak calcein labelling (C), condensed chromatin (D) or pronounced membrane blebbing (A and C). The morphological alterations are indicative of the induction of apoptotic and/or necrotic events induced by *t*-BHP in accordance with the literature [20]. The results also indicate that among the nitrogen compounds tested only FMA762 and FMA796 are able to prevent almost completely *t*-BHP-induced alterations of H9c2 cells. In fact, no evidence of necrotic cells could be found in the cell populations treated with FMA762 or FMA796 plus *t*-BHP. For FMA4, and especially for FMA7, a slight protective effect was also observed, although not as powerful as for FMA762 or FMA796. These results are indicative of a superior protective effect of FMA762 and FMA796 against *t*-BHP-induced morphological changes and constitute a

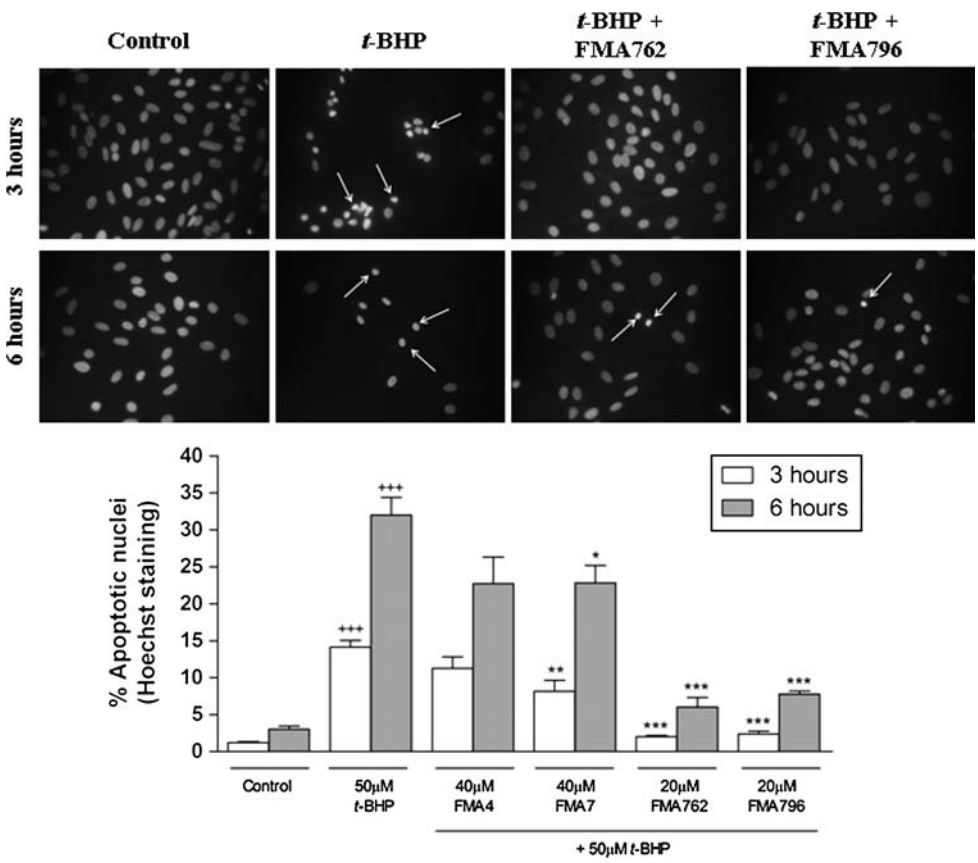

Fig. 4 Quantification of apoptotic nuclei after labelling cells with the fluorescent dye Hoechst 33342. *Top panel*: Representative images, obtained by fluorescence microscopy of Hoechst-labelled nuclei of H9c2 cells after treatment with *t*-BHP and the nitrogen compounds (in this case, only FMA762 and FMA796 are represented) for 3 and 6 h. *Arrows* indicate nuclei showing condensed chromatin, characteristic of apoptosis. *Bottom panel*: The number of apoptotic nuclei were counted and expressed as the percentage of total cells counted (approximately 200 cells per coverslip). For each *bar*, the mean ± SEM for five independent experiments is represented. $^{+++}$ $P \leq 0.001$, compared to respective control; * $P \leq 0.05$, ** $P \leq 0.01$, *** $P \leq 0.001$, compared to 50 μM *t*-BHP (for the respective time period)

strong evidence of the compounds' role in the apoptotic cascade of events.

Determination of the Compounds' Effects on Mitochondrial Membrane Potential

Changes in mitochondrial membrane potential ($\Delta\psi$) were assessed after loading the cells with the membrane-permeable cationic fluorophore TMRM. In order to reduce the risk of generating artefacts in the determination of fluorescence intensity due to probe release to the cytosol, two quantification parameters were used: cell mean fluorescence and fSD. Results in Fig. 6 (*bottom panel*) show that in the presence of *t*-BHP there is a decrease in both parameters relatively to control cells, which is indicative of the depolarization of mitochondria. The simultaneous incubation of *t*-BHP with the compounds FMA762 and FMA796 significantly prevented mitochondrial depolarization, as demonstrated by the values obtained in these conditions, which are similar to the control. In addition, the nitrogen compounds, by themselves, did not cause any changes in the mitochondrial $\Delta\psi$ as measured by the two parameters. The effects obtained with CCCP, a protonophore that induces the collapse of mitochondrial membrane potential [27], validated the assay. The representative images on the top panel of the same figure illustrate the observations described.

Results in this figure indicate that mitochondrial depolarization is a component of myoblast cell death induced by *t*-BHP and that the compounds in study also act by preserving mitochondrial transmembrane electric potential.

Assessment of Caspases-3 and -9 Activities

The loss of mitochondrial membrane potential, as well as cell blebbing, and redistribution of lipids in the outer plasma membrane are some of the phenotypic characteristics of apoptotic cell death that can be mediated by caspases activation [28].

As depicted in Fig. 7a, *t*-BHP induced the activation of caspase-3, an effector caspase, as indicated by the almost threefold increase in the cleavage of its substrate. Caspase-3 activation seems to be mediated by the mitochondrial apoptotic pathway, since caspase-9 activation was also observed (Fig. 7b). Confirming previous data, FMA762 and FMA796 were able to prevent the activation of both caspases tested in a statistically significant manner, which is indicative of a protective role for the nitrogen compounds against *t*-BHP-induced apoptotic cell death, particularly by an involvement in the mitochondrial cascade.

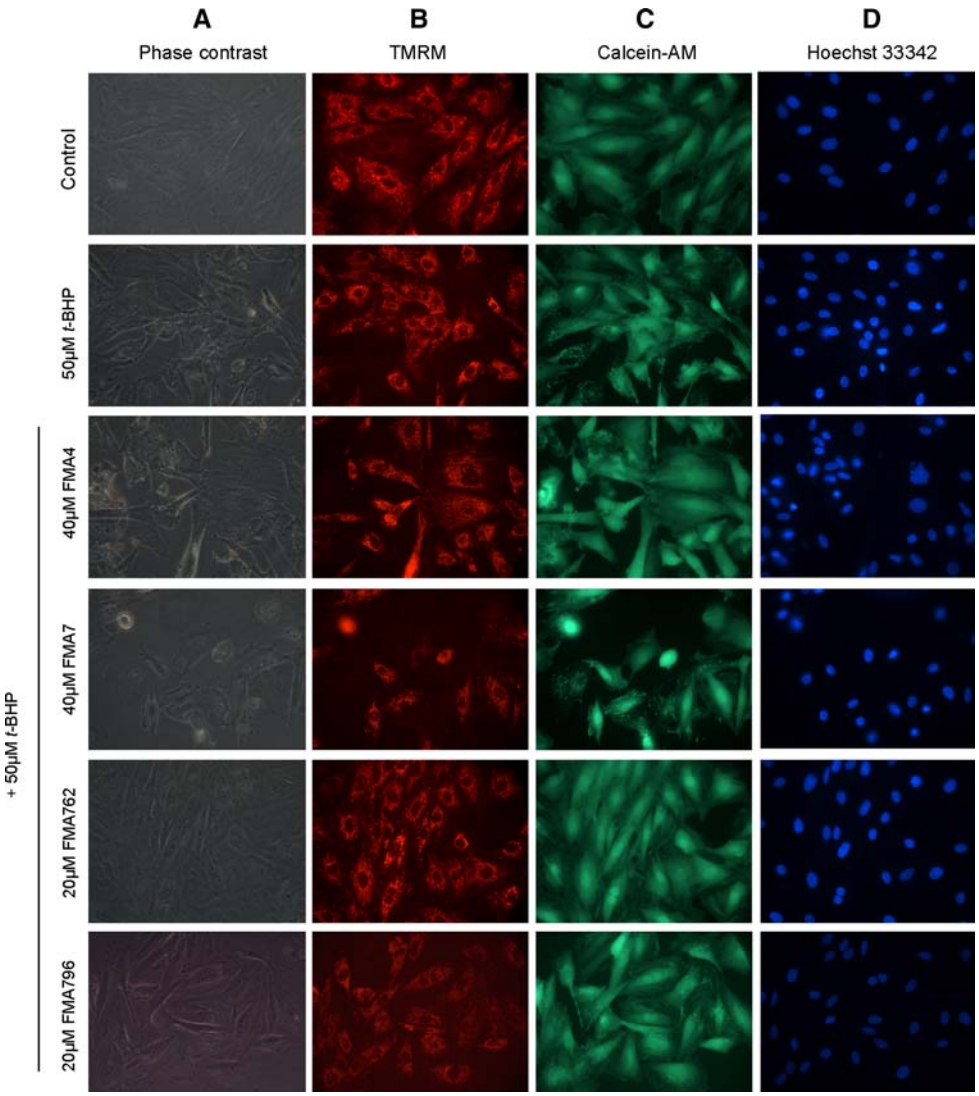

Fig. 5 Protection against *t*-BHP—induced alterations in cellular and mitochondrial morphology. H9c2 cells were incubated for 3 h in the presence of 50 μM *t*-BHP with or without the nitrogen compounds. Cells were then labelled with 100 nM TMRM, 300 nM Calcein-AM and 1 μg ml^{-1} Hoechst 33342. *Images* are representative of five independent experiments

Expression of Pro-Apoptotic Proteins

Given the protective effects of the compounds on caspases activation (Fig. 7) and on apoptotic-like morphological changes induced by *t*-BHP in H9c2 cells, namely at the mitochondrial and nuclear levels (Fig. 5), we tried to identify more specific targets, especially proteins known to activate apoptotic pathways, such as p53, Bax and AIF.

As observed in Fig. 8a, *t*-BHP induces an increase in the expression of the transcription factor p53, known to lead to the expression of proteins that prevent cell division and cause apoptosis [28]. These results are also in accordance with data obtained by others for doxorubicin-induced myocyte cell death [29]. This activation of p53 was significantly reversed in the presence of FMA762 and FMA796. Likewise, the increase in Bax expression observed in the presence of *t*-BHP (Fig. 8b) was also prevented by the action of the nitrogen compounds. Bax acts downstream of p53 and is responsible for the permeabilization of the outer mitochondrial membrane, leading to the release of pro-apoptotic proteins [28]. Therefore, these results confirm that the nitrogen compounds may prevent DNA damage by the pro-oxidants, increased expression of p53 and its targets and subsequently the activation of the apoptotic mitochondrial pathway.

Apoptosis may also be induced by a caspase-independent pathway, namely by the translocation of the apoptosis-inducing factor (AIF) from mitochondria to the nucleus, where it interacts with nucleic acids, causing chromatin condensation and DNA fragmentation [30]. As it is shown in Fig. 8c, *t*-BHP led to an increase in the expression of AIF in the nuclear extracts of H9c2 cells, which was once again significantly prevented by FMA762 and FMA796.

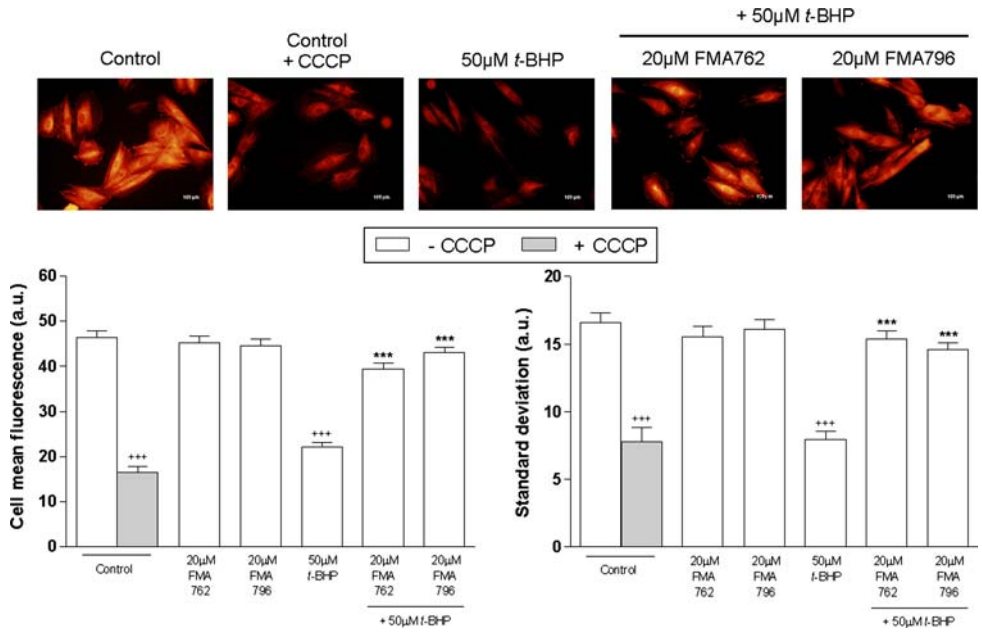

Fig. 6 Effects of the compounds on mitochondrial membrane depolarization. Cells were loaded with 2 μM TMRM 30 min prior to the end of the 3 h incubation in the presence of *t*-BHP and of the nitrogen compounds. CCCP was used to induce the complete depolarization of the inner mitochondrial membrane. *Top panel*: Images representative of each condition. *Bottom panel*: quantification of mitochondrial membrane potential, using two different parameters: cell mean fluorescence intensity and standard deviation (referred as fSD in the text). Each *bar* represents the mean ± SEM for at least four independent experiments. $^{+++}$ $P \leq 0.001$, compared to control cells in the absence of CCCP; *** $P \leq 0.001$, compared to 50 μM *t*-BHP

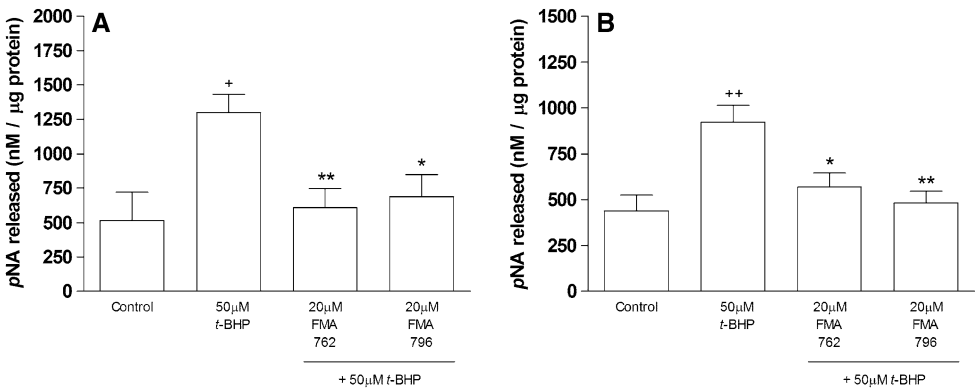

Fig. 7 Activities of caspases-3 (**a**) and -9 (**b**). H9c2 cells were incubated in the presence of both nitrogen compounds and *t*-BHP for 3 h. Each *bar* represents the mean ± SEM for at least three independent experiments. $^{+}$ $P \leq 0.05$, compared to control cells; * $P \leq 0.05$, ** $P \leq 0.01$, in comparison with 50 μM *t*-BHP

Measurement of Intracellular Reactive Oxygen Species

Our previous results with the same compounds in a neuronal cell model have indicated their important ROS/RNS scavenging activity. By its turn, *t*-BHP is a pro-oxidant agent widely used as an inducer of oxidative stress [26, 31]. So, the effect of the compounds on *t*-BHP-induced oxidative stress on H9c2 cells was assessed by fluorescence microscopy, through the detection of oxidized dichlorofluorescein (DCF) form.

As expected, cell treatment with 50 μM *t*-BHP induces an increase in intracellular oxidative stress, as demonstrated by the increase in the cell mean fluorescence after 3 h incubation with the oxidant (Fig. 9). The fluorescence increase is attenuated in the presence of three of the four compounds studied, namely FMA7, FMA762 and FMA796. Once again, in the case of FMA762 and FMA796, oxidative stress was reduced to values similar to the control for the concentration (20 μM) at which they proved protection in all the endpoints tested previously. These results are in agreement with previous data obtained in PC12 cells [12].

In a cell-free system, the nitrogen compounds confirmed their antiradical activity, namely regarding their superoxide anion ($O_2^{\bullet -}$) scavenging ability evaluated through the use of a non-enzymatic (PMS/NADH) and an enzymatic (xanthine/xanthine oxidase) system to generate this radical.

As it can be observed in Fig. 10a, FMA762 and FMA796 are able to scavenge superoxide radicals generated by the

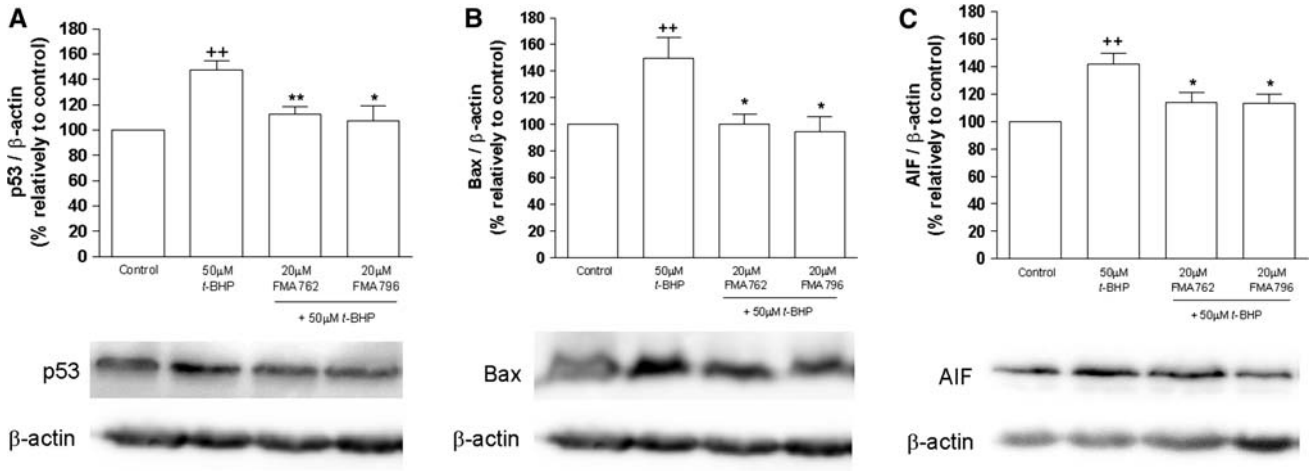

Fig. 8 Effects of the test compounds on the expression of the pro-apoptotic proteins **a** p53, **b** Bax and **c** apoptosis-inducing factor (AIF). Cells were treated with *t*-BHP and the nitrogen compounds either for 6 h (Bax and p53) or 15 h (AIF). For the analysis of Bax and p53 expression, total extracts were used, while extracts of the nuclear fractions were prepared to assess AIF expression. p53, Bax and AIF were identified as protein bands of 53, 20 and 57 KDa, respectively, and their expression calculated relatively to *β*-actin. Each *bar* represents the mean ± SEM for at least five independent experiments. $^{++}$ $P \leq 0.01$, compared to control; * $P \leq 0.05$, ** $P \leq 0.01$ compared with 50 μM *t*-BHP

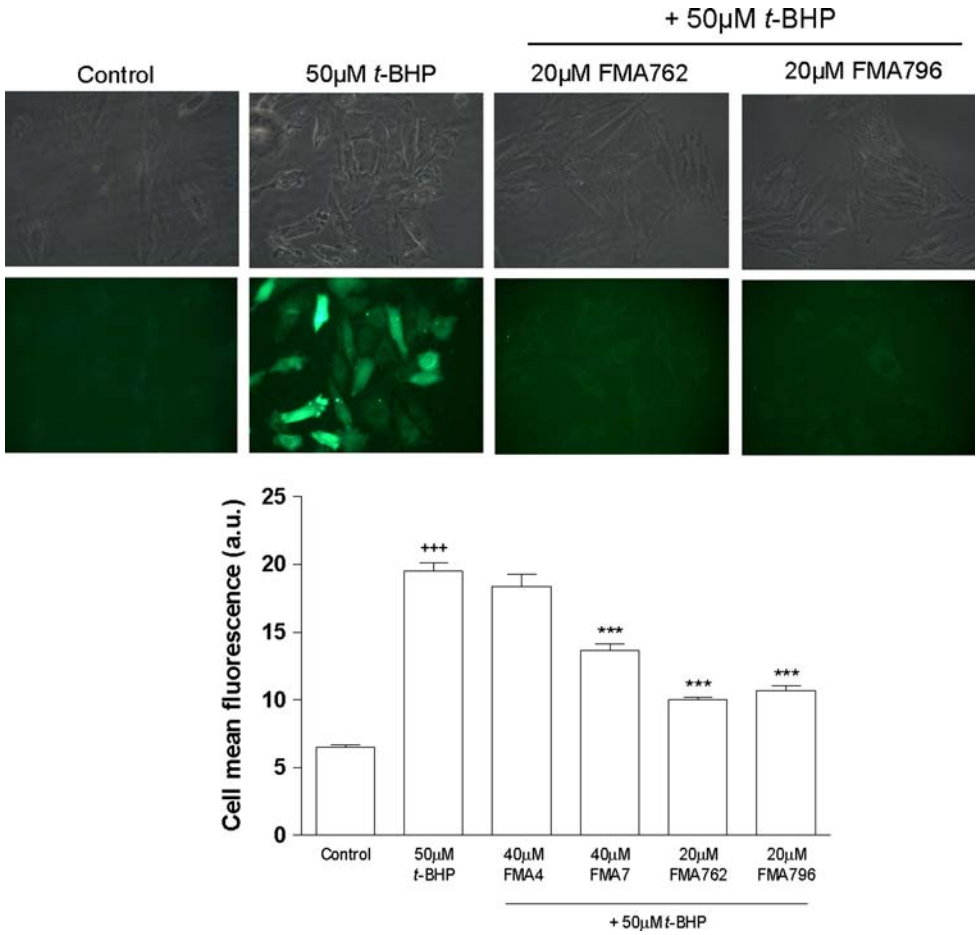

Fig. 9 Effects of the compounds on *t*-BHP-induced intracellular oxidative stress. H9c2 cells were incubated in the presence of *t*-BHP and the nitrogen compounds for 3 h. Increase in intracellular oxidative stress was detected by oxidation of the fluorescent probe dichlorofluorescein. *Top panel*: Representative images, obtained by fluorescence microscopy, of cells treated with *t*-BHP and the nitrogen compounds FMA762 and FMA796. *Bottom panel*: Quantification of DCF fluorescence intensity. At least five fields per sample were analysed in each experiment. For each *bar* is represented the mean ± SEM for five independent experiments. $^{+++}$ $P \leq 0.001$, compared with control, *** $P \leq 0.001$, relatively to *t*-BHP

PMS/NADH system, with IC_{50} values of 7.01 ± 0.80 and 15.44 ± 0.68 μM, respectively. This data was also confirmed by determining the effect of the nitrogen compounds on superoxide generated by the xanthine/xanthine oxidase system (Fig. 10b), which gave IC_{50} values of 1.61 ± 0.11 and 2.45 ± 0.14 μM for FMA762 and FMA796,

respectively, that are of the same order of magnitude. Nevertheless, this last approach, using the xanthine/xanthine oxidase system is more suitable in a cellular context.

The results obtained by both systems indicate the ability of the compounds to directly scavenge superoxide radicals. The low IC_{50} values obtained were somewhat expected, according to our previous work [12] and confirm the high antioxidant activity of the nitrogen compounds.

Discussion

Oxidative stress has been reported to be involved in several cardiomyopathies [32], namely by inducing modifications in phospholipids and proteins, and therefore causing abnormalities in the myocyte function.

Recently, we have been characterizing the antioxidant potential of novel nitrogen compounds against events where oxidative stress is involved, trying to find possible action targets for neurodegeneration prevention. The structures of these novel molecules yield them a superior activity as antioxidants, in comparison with other commonly used molecules, such as Trolox and quercetin, as previously described [12, 33]. In this particular study, we evaluated the ability of the test compounds to protect against oxidative injury on a cell model for cardiomyocytes, the H9c2 cell line, with a particular interest in finding an intracellular action target.

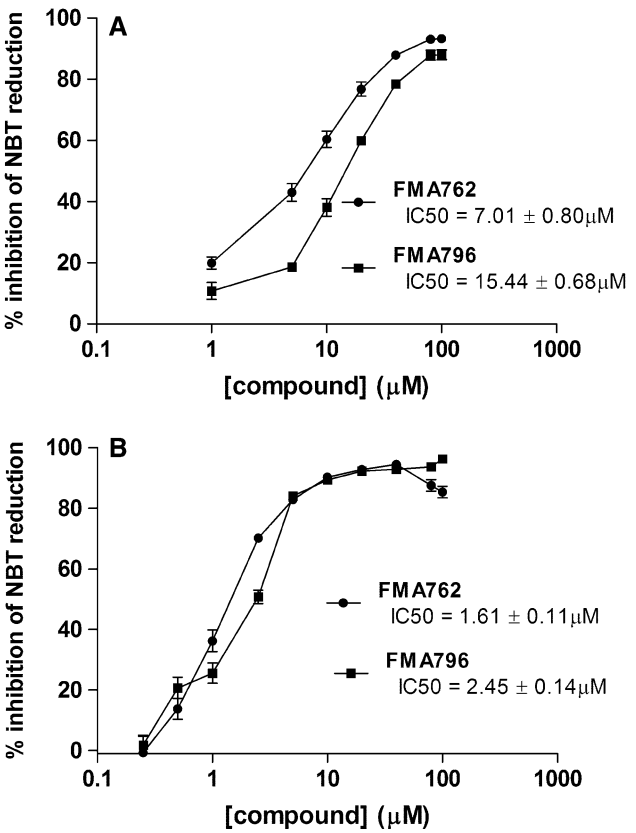

Fig. 10 Effect of the nitrogen compounds on NBT reduction induced by superoxide radical generated in **a** an NADH/PMS system or **b** a xanthine/xanthine oxidase system. The IC_{50} values were calculated from the represented curves, as the concentration needed to inhibit the reduction of NBT by 50%. For each concentration, the mean ± SEM is represented, considering the results obtained in at least three different experiments

We observed that none of the nitrogen compounds interfered with normal H9c2 cell proliferation at least up to 96 h. In the case of FMA762 and FMA796, this was only observed for concentrations up to 75 μM. Nevertheless, it should be taken into account that 75 μM is a concentration about 20-fold higher than the IC_{50} values previously determined by the DPPH discolouration assay [12] and therefore may never be reached in vivo.

At the concentrations tested (20 μM for FMA4 and FMA7, and 5 μM for FMA762 and FMA796) and after a 6-h incubation period, the morphological changes induced by *t*-BHP to H9c2 cells did not seem to be reverted by incubating cells with FMA4, and FMA7, which appeared to only have a slight protective effect, since apoptosis (cells accumulating green calcein fluorescence, but presenting chromatin condensation and loss of mitochondrial membrane potential as depicted by TMRM labelling) and necrosis (loss of membrane integrity and decrease or complete dissipation of mitochondrial membrane potential) still occurred. On the other hand, in the presence of FMA762 and FMA796, only a few apoptotic cells were identified and no necrotic cells could be visualized, indicating the higher protective action of these two compounds.

Mitochondrial membrane depolarization has been described as one of the events that occurs as a response to oxidant stimuli [34]. In agreement with that, we observed a loss of mitochondrial $\Delta\psi$ in the presence of *t*-BHP, as indicated by a decrease in TMRM mean fluorescence inside mitochondria. The evaluation of both mean fluorescence intensity and the fSD parameter (according to Brennan et al. [22]) shows that FMA762 and FMA796 were able to prevent *t*-BHP-induced mitochondrial depolarization. These results assume great relevance given the importance of mitochondria in the regulation of intracellular pathways leading to cell death. In fact, the depolarization resulting from mitochondrial $\Delta\psi$ disruption leads to an increase in the permeability of the outer mitochondrial membrane, which causes the release of several pro-apoptotic factors (e.g., cytochrome *c*, AIF, among others) from mitochondria [35].

Apoptosis is an active cell death process that has been recognized as essential to the pathogenesis of cardiovascular diseases [10]. In this study, the tested nitrogen compounds, namely FMA762 and FMA796, proved their effectiveness in preventing the activation of both caspases

3 and 9, involved in the mitochondria-mediated apoptotic pathway. The results demonstrate the ability of the compounds to act on the intracellular signalling cascade leading to apoptotic cell death, most likely by preventing mitochondrial disruption.

It is generally accepted that the tumour suppressor protein p53 is activated by DNA damage, leading to an increase in the expression of genes that prevent cell division and cause apoptosis. This may result in the activation of pro-apoptotic Bcl-2 family members, such as Bax, causing the permeabilization of the outer mitochondrial membrane and subsequent activation of the above mentioned mitochondrial-mediated apoptotic pathway [36]. The results presented show that FMA762 and FMA796 decreased *t*-BHP-induced increase in p53 and Bax protein levels, indicating that their protective effects may precede mitochondria depolarization and subsequent activation of caspases.

Additionally, we determined a possible action of the compounds on the caspase-independent pathway, mediated by the apoptosis-inducing factor (AIF). The AIF is a mitochondrial flavoprotein oxidoreductase that is translocated to the cytosol and then to the nucleus, where it interacts with nucleic acids [30]. Here, we observed an increased AIF presence in nuclear extracts from *t*-BHP-treated cells, which was prevented once again by FMA762 and FMA796. These results suggest that the test compounds may act at different mechanisms of apoptotic signalling. Nevertheless, the role of the AIF on *t*-BHP-induced toxicity on H9c2 myoblasts is currently under investigation.

The high compounds' ROS scavenging properties shown in our previous studies suggested that the protective role of the compounds on all these events may be mediated precisely by their ROS scavenging activity. In fact, they were able to significantly protect H9c2 cells against intracellular oxidative stress induced by *t*-BHP, as expected. We obtained additional evidence for their ability to scavenge the superoxide anion ($O_2^{\bullet -}$) in two cell-free systems. Although this radical is not regarded as highly reactive in a cellular context due to its inability to cross-lipid membranes, it is formed during many metabolic processes and can easily yield more reactive species, such as hydrogen peroxide and molecular oxygen by the action of superoxide dismutase [32]. Therefore, the significant superoxide scavenging activity demonstrated by the new compounds, namely FMA762 and FMA796 (indicated by their low IC_{50} values), can assume great relevance.

We conclude that the new nitrogen compounds in study clearly protect H9c2 cells against oxidative stress-induced damage. FMA762 and FMA796, which differ from the other two (FMA4 and FMA7) by the presence of three hydroxyl groups within the phenol ring, revealed a superior profile of protection, since they were able to protect cells to a higher extent and at lower concentrations. In addition, FMA762 and FMA796 seem to be able to interfere in the regulation of intracellular signalling mechanisms leading to apoptotic cell death, namely those mediated by mitochondria. This was confirmed by their ability to overcome *t*-BHP-induced morphological changes in the mitochondrial network, loss of mitochondrial membrane potential, caspases activation and increased expression of pro-apoptotic proteins leading to induction of both caspase-dependent and -independent pathways. It is also worth noticing that the beneficial effects occur for concentrations at which toxicity is not apparent.

The overall results obtained with these compounds are very promising in the context of the development of novel antioxidant agents capable of preventing cardiac injury directly related to free radical production. However, care should be taken before extrapolating these results to the clinical practice. In fact, for the past three decades, many studies have reported several agents able to protect the ischaemic myocardium in experimental in vitro and in vivo models, but have failed in the translation to the clinic [37]. Differences in methodology and biology between the preclinical and clinical studies may be on the basis of the negative clinical trials [38]. Nevertheless, other studies have already demonstrated that some of these agents, effective in vitro, are also able to limit myocardial ischaemia/reperfusion in humans [39, 40]. So, although this work intended to be a first approach to evaluate the effects of the nitrogen compounds as cardioprotectors, and further studies (namely in animal models) need to be conducted to determine their real effects at the myocardium level, a potential cardioprotective role should not be discarded for these compounds. In fact, the novel results presented in this cardiomyocyte model represent an advance in the study of these compounds as potential therapeutic agents, since it widens their spectrum of action, while pointing out their targets within the cell. Furthermore, these results can be added up to the data collected in previous models for neurodegenerative diseases, increasing their relevance even further.

Acknowledgments JPS is supported by the Portuguese Foundation for Science and Technology (FCT), Grant SFRH/BD/17174/2004. The present work was supported by FCT research Grant PTDC/QUI/64358/2006. We want to thank Prof. Fernanda Proença, from the Department of Chemistry, University of Minho, for kindly supplying the synthetic nitrogen compounds used.

References

1. Sgobbo, P., Pacelli, C., Grattagliano, I., Villani, G., & Cocco, T. (2007). Carvedilol inhibits mitochondrial complex I and induces resistance to H_2O_2-mediated oxidative insult in H9c2 myocardial cells. *Biochimica et Biophysica Acta, 1767*, 222–232.

2. Giordano, F. J. (2005). Oxygen, oxidative stress, hypoxia, and heart failure. *Journal of Clinical Investigation, 115*, 500–508.
3. Sam, F., Kerstetter, D. L., Pimental, D. R., Mulukutla, S., Tabaee, A., Bristow, M. R., et al. (2005). Increased reactive oxygen species production and functional alterations in antioxidant enzymes in human failing myocardium. *Journal of Cardiac Failure, 11*, 473–480.
4. Kaiserova, H., Simunek, T., van der Vijgh, W. J. F., Bast, A., & Kvasnickova, E. (2007). Flavonoids as protectors against doxorubicin cardiotoxicity: Role of iron chelation, antioxidant activity and inhibition of carbonyl reductase. *Biochimica et Biophysica Acta, 1772*, 1065–1074.
5. Nakamura, K., Kusano, K., Nakamura, Y., Kakishita, M., Ohta, K., Nagase, S., et al. (2002). Carvedilol decreases elevated oxidative stress in human failing myocardium. *Circulation, 105*, 2867–2871.
6. Zhao, K., Zhao, G. M., Wu, D., Soong, Y., Birk, A. V., Schiller, P. W., et al. (2004). Cell-permeable peptide antioxidants targeted to inner mitochondrial membrane inhibit mitochondrial swelling, oxidative cell death, and reperfusion injury. *Journal of Biological Chemistry, 279*, 34682–34690.
7. Wallace, K. B. (2007). Adriamycin-induced interference with cardiac mitochondrial calcium homeostasis. *Cardiovascular Toxicology, 7*, 101–107.
8. Isomoto, S., Kawakami, A., Arakaki, T., Yamashita, S., Yano, K., & Ono, K. (2006). Effects of antiarrhythmic drugs on apoptotic pathways in H9c2 cardiac cells. *Journal of Pharmacological Sciences, 101*, 318–324.
9. Petrosillo, G., Ruggiero, F. M., & Paradies, G. (2003). Role of reactive oxygen species and cardiolipin in the release of cytochrome c from mitochondria. *FASEB Journal, 17*, 2202–2208.
10. Reeve, J. L. V., Szegezdi, E., Logue, S. E., Chonghaile, T. N., O'Brien, T., Ritter, T., et al. (2007). Distinct mechanisms of cardiomyocyte apoptosis induced by doxorubicin and hypoxia converge on mitochondria and are inhibited by Bcl-XL. *Journal of Cellular and Molecular Medicine, 11*, 509–520.
11. Silva, J. P., Areias, F. M., Proença, M. F., & Coutinho, O. P. (2006). Oxidative stress protection by newly synthesized nitrogen compounds with pharmacological potential. *Life Science, 78*, 1256–1267.
12. Silva, J. P., Proença, M. F., & Coutinho, O. P. (2008). Protective role of new nitrogen compounds on ROS/RNS-mediated damage to PC12 cells. *Free Radical Research, 42*, 57–69.
13. Marczin, N., El-Habashi, N., Hoare, G. S., Bundy, R. E., & Yacoub, M. (2003). Antioxidants in myocardial ischemia-reperfusion injury: Therapeutic potential and basic mechanisms. *Archives of Biochemistry and Biophysics, 420*, 222–236.
14. Haramaki, N., Stewart, D. B., Aggarwai, S., Ikeda, H., Reznick, A. Z., & Packer, L. (1998). Networking antioxidants in the isolated rat heart are selectively depleted by ischemia-reperfusion. *Free Radical Biology and Medicine, 25*, 329–339.
15. Areias, F. M. (2006). Novos compostos heterocíclicos de azoto com unidades fenólicas: síntese e actividade biológica, Ph.D. Thesis. University of Minho, Braga, Portugal. Available online at: http://hdl.handle.net/1822/5941.
16. Kimes, B. W., & Brandt, B. L. (1976). Properties of a clonal muscle cell line from rat heart. *Experimental Cell Research, 98*, 367–381.
17. L'Ecuyer, T., Horenstein, M. S., Thomas, R., & Heide, R. V. (2001). DNA damage is an early event in doxorubicin-induced cardiac myocyte death. *American Journal of Physiology, 74*, 370–379.
18. Dangel, V., Giray, J., Ratge, D., & Wisser, H. (1996). Regulation of beta-adrenoceptor density and mRNA levels in the rat heart cell-line H9c2. *Biochemical Journal, 317*, 925–931.
19. Papazisis, K. T., Geromichalos, G. D., Dimitriadis, K. A., & Kortsaris, A. H. (1997). Optimization of the sulforhodamine B colorimetric assay. *Journal of Immunological Methods, 208*, 151–158.
20. Sardão, V. A., Oliveira, P. J., Holy, J., Oliveira, C. R., & Wallace, K. B. (2007). Vital imaging of H9c2 myoblasts exposed to *tert*-butylhydroperoxide—characterization of morphological features of cell death. *BMC Cell Biology, 8*, 11–27.
21. Ehrenberg, B., Montana, V., Wei, M. D., Wuskell, J. P., & Loew, L. M. (1988). Membrane potential can be determined in individual cells from the nernstian distribution of cationic dyes. *Biophysical Journal, 53*, 785–794.
22. Brennan, J. P., Berry, R. G., Baghai, M., Duchen, M. R., & Shattock, M. J. (2006). FCCP is cardioprotective at concentrations that cause mitochondrial oxidation without detectable depolarisation. *Cardiovascular Research, 72*, 322–330.
23. Serafim, T. L., Matos, J. A. C., Sardão, V. A., Pereira, G. C., Branco, A. F., Pereira, S. L., et al. (2008). Sanguinarine cytotoxicity on mouse melanoma K1735-M2 cells—Nuclear vs. mitochondrial effects. *Biochemical Pharmacology, 76*, 1459–1475.
24. Valentão, P., Fernandes, E., Carvalho, F., Andrade, P. B., Seabra, R. M., & Bastos, M. L. (2001). Antioxidant activity of *Centaurium erythraea* infusion evidenced by its superoxide radical scavenging and xanthine oxidase inhibitory activity. *Journal of Agricultural and Food Chemistry, 49*, 3476–3479.
25. Alia, M., Ramos, S., Mateos, R., Bravo, L., & Goya, L. (2005). Response of the antioxidant defense system to *tert*-butyl hydroperoxide and hydrogen peroxide in a human hepatoma cell line (HepG2). *Journal of Biochemical and Molecular Toxicology, 19*, 119–128.
26. Pias, E. K., & Aw, T. Y. (2002). Early redox imbalance mediates hydroperoxide-induced apoptosis in mitotic competent undifferentiated PC12 cells. *Cell Death and Differentiation, 9*, 1007–1016.
27. Lim, M. L. R., Minamikawa, T., & Nagley, P. (2001). The protonophore CCCP induces mitochondrial permeability transition without cytochrome c release in human osteosarcoma cells. *FEBS Letters, 503*, 69–74.
28. Beere, H. M. (2005). Death versus survival: Functional interaction between the apoptotic and stress-inducible heat shock protein pathways. *Journal of Clinical Investigation, 115*, 2633–2639.
29. Sardão, V. A., Oliveira, P. J., Holy, J., Oliveira, C. R., & Wallace, K. B. (2009). Doxorubicin-induced mitochondrial dysfunction is secondary to nuclear p53 activation in H9c2 cardiomyoblasts. *Cancer Chemotherapy and Pharmacology*, *64*, 811–827.
30. Lorenzo, H. K., & Susin, S. A. (2007). Therapeutic potential of AIF-mediated caspase-independent programmed cell death. *Drug Resistance Updates, 10*, 235–255.
31. Ahmed-Choudhury, J., Orsler, D. J., & Coleman, R. (1998). Hepatobiliary effects of tertiary-butylhydroperoxide (tBOOH) in isolated rat hepatocyte couplets. *Toxicology and Applied Pharmacology, 152*, 270–275.
32. Valko, M., Leibfritz, D., Moncol, J., Cronin, M. T. D., Mazur, M., & Telser, J. (2007). Free radicals and antioxidants in normal physiological functions and human disease. *International Journal of Biochemistry and Cell Biology, 39*, 44–84.
33. Silva, J. P., Gomes, A. C., Proença, F., & Coutinho, O. P. (2009). Novel nitrogen compounds enhance protection and repair of oxidative DNA damage in a neuronal cell model: Comparison with quercetin. *Chemico-Biological Interactions, 181*, 328–337.
34. Orrenius, S., Gogvadze, V., & Zhivotovsky, B. (2007). Mitochondrial oxidative stress: Implications for cell death. *Annual Review of Pharmacology and Toxicology, 47*, 143–183.
35. Haidara, K., Morel, I., Abaléa, V., Barré, M. G., & Denizeau, F. (2002). Mechanism of *tert*-butylhydroperoxide induced apoptosis

in rat hepatocytes: Involvement of mitochondria and endoplasmic reticulum. *Biochimica et Biophysica Acta, 1542,* 173–185.
36. L'Ecuyer, T., Sanjeev, S., Thomas, R., Novak, R., Das, L., Campbell, W., et al. (2006). DNA damage is an early event in doxorubicin-induced cardiac myocyte death. *American Journal of Physiology, 291*, 1273–1280.
37. Bolli, R., Becker, L., Gross, G., Mentzer, R., Jr., Balshaw, D., & Lathrop, D. A. (2004). Myocardial protection at a crossroads: The need for translation into clinical therapy. *Circulation Research, 95*, 125–134.
38. Dirksen, M. T., Laarman, G. J., Simoons, M. L., & Duncker, D. J. G. M. (2007). Reperfusion injury in humans: A review of clinical trials on reperfusion injury inhibitory strategies. *Cardiovascular Research, 74*, 343–355.
39. Mahaffey, K. W., Puma, J. A., Barbagelata, N. A., DiCarli, M. F., Leesar, M. A., Browne, K. F., et al. (1999). Adenosine as an adjunct to thrombolytic therapy for acute myocardial infarction: Results of a multicenter, randomized, placebo-controlled trial: The acute myocardial infarction study of adenosine (Amistad) trial. *Journal of the American College of Cardiology, 34*, 1711–1720.
40. Mentzer, R. M., Jr., Bartels, C., Bolli, R., Boyce, S., Buckberg, G. D., Chaitman, B., et al. (2008). Sodium-hydrogen exchange inhibition by cariporide to reduce the risk of ischemic cardiac events in patients undergoing coronary artery bypass grafting: Results of the expedition study. *Annals of Thoracic Surgery, 85*, 1261–1270.